

Gold(I) and Silver(I)  $\pi$ -Complexes with Unsaturated Hydrocarbons

Petr Motloch,\* Juraj Jašík, and Jana Roithová\*

 Cite This: *Organometallics* 2021, 40, 1492–1502

Read Online

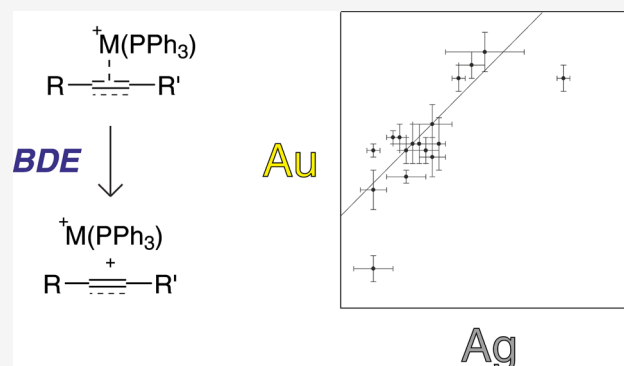
ACCESS |

Metrics &amp; More

Article Recommendations

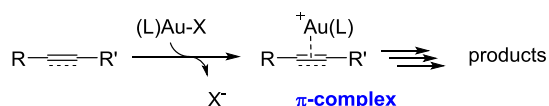
Supporting Information

**ABSTRACT:** Gold  $\pi$ -complexes have been studied largely in the past 2 decades because of their role in gold-catalyzed reactions. We report an experimental and theoretical investigation of the interaction between a wide range of unsaturated hydrocarbons (alkanes, alkynes, alkadienes, and allenes) and triphenylphosphine-gold(I), triphenylphosphine-silver(I), and acetonitrile-silver(I) cations. The bond dissociation energies of these complexes were determined by mass spectrometry collision-induced dissociations and their structures were studied by density functional theory calculations and infrared photodissociation spectroscopy. The results show that with the same phosphine ligand, gold binds stronger to the  $\pi$ -ligands than silver and thereby activates the unsaturated bond more effectively. Ligand exchange of phosphine by acetonitrile at the silver complexes  $\pi$ -increases the binding energy as well as the activation of the  $\pi$ -ligands. We also show that the substitution of an



## INTRODUCTION

Gold catalysis is one of the important sub-topics of current homogeneous catalysis.<sup>1–15</sup> Its main advantage is a mild and chemoselective activation of C–C multiple bonds for a nucleophile attack. Cationic two-coordinate  $\pi$ -complexes of gold with unsaturated hydrocarbons are considered as initial reaction intermediates in almost every reaction catalyzed by cationic gold(I) (Scheme 1) and therefore they attract

Scheme 1. Proposed Role of  $\pi$ -Complexes in Gold Catalysis

substantial attention.<sup>16,17</sup> Brooner and Widenhoefer highlighted the importance of those complexes in gold(I) catalysis with a focus on their structure, bonding, and ligand exchange behavior.<sup>18</sup> Hashmi and Jones analyzed the same topic in their subsequent reviews.<sup>19,20</sup>

The cationic gold(I) catalysts are usually prepared *in situ* from their gold chloride precursors by an anion exchange with silver salts. Silver salts are typically added in excess; thus, possible (co)catalytic effects cannot be excluded. We have shown that excess silver cations did not affect the kinetics of a simple gold-catalyzed nucleophilic addition to alkynes.<sup>21</sup> However, an example of a “silver effect” was presented by Shi and co-workers in 2012.<sup>22</sup> They showed that the simultaneous presence of both gold and silver species was crucial for several reactions to proceed. Since this contribution,

the discussion on the silver effect has increased significantly.<sup>23–29</sup>

Our research group has already used the combination of mass spectrometry, ion spectrometry, and theoretical calculations for determining of possible silver effects in gold catalysis.<sup>30,31</sup> The cationic nature of the reactive gold(I) and silver(I) complexes with  $\pi$ -ligands allows their detection by electrospray ionization (ESI) mass spectrometry. Once isolated in the gas phase, their thermodynamic properties can be assessed, their bimolecular reactions can be studied, and also their optical absorption spectra can be measured.<sup>32–35</sup> This work continues in the investigation of cationic  $\pi$ -complexes of silver and gold complexes with ancillary ligands with a wide range of unsaturated hydrocarbons. We aim at a systematic comparison of binding energies and modes of activation of hydrocarbons in gold and silver  $\pi$ -complexes. We use triphenylphosphine as the main ancillary ligand because it is among the most applied ligands in gold catalysis.<sup>36</sup> For a long time, the triphenylphosphine–gold  $\pi$ -complexes were considered unstable in solution.<sup>37,38</sup> However, we have recently shown that these complexes are much more stable than what was previously published and we were also able to characterize them by X-ray for the first time.<sup>39</sup> Other silver(I) and gold(I)

Received: March 9, 2021

Published: May 6, 2021



$\pi$ -complexes utilizing phosphines and other ligands were characterized previously as well.<sup>40–48</sup>

This work aims at the comparison of silver(I) and gold(I)  $\pi$ -complexes with the same supporting ligand to clearly distinguish the direct effect of the noble metals. In addition, a change of the supporting ligand on silver simulates the more realistic situation in solution. We focus our attention on the strength of the coordination bond, the lengthening of the  $\pi$ -bond, and the mode of activation.

**Experimental and Computational Details.** The experiments were performed with a Paul-type ion-trap mass spectrometer LCQ Deca (ThermoQuest). Ions were generated by ESI from dichloromethane solutions of unsaturated hydrocarbon and either AgSbF<sub>6</sub> with an additional ligand (PPh<sub>3</sub>, CH<sub>3</sub>CN) or Au(PPh<sub>3</sub>)Cl activated by AgSbF<sub>6</sub> (see the [Supporting Information](#) for details). Conditions for ESI: the nebulizer gas was nitrogen, the spraying voltage was 5–6 kV, the heated capillary was kept at 150–200 °C, and the flow rate of the solution was set to 0.3 mL·h<sup>-1</sup>. Mass-selection was done with a uniform isolation width of 1.6 amu. Collision activation in the collision-induced dissociation (CID) experiments was achieved through radiofrequency excitation (30 ms) followed by collisions with the helium buffer gas (the pressure of helium within the ion trap was  $\sim 10^{-3}$  mbar). The trapping parameter  $q_z$  was 0.25. The “normalized” collision energy scale used in LCQ ion traps can be calibrated and transformed to the center-of-mass collision energies.<sup>49</sup> Therefore, the appearance energies of the fragments in collision-energy resolved experiments correspond to the bond dissociation energies (BDEs).<sup>50–52</sup> All experiments were measured six times on at least two different days in order to eliminate possible systematic errors.

All calculations were performed with a Gaussian 09 package.<sup>53</sup> Structures were optimized by density functional theory method mPW1PW91.<sup>54</sup> The basis set cc-pVTZ was used for H, C, N, O, P, and Cl atoms.<sup>55</sup> Pseudopotential LanL2DZ for Ag and Au was used to account for relativistic effects.<sup>56</sup> The combination of both is denoted as cc-pVTZ/LanL2DZ in the following. Final binding energies were corrected for the basis-set superposition error (BSSE).<sup>57</sup> All reported structures were confirmed by the analysis of the corresponding Hessian matrices to be genuine minima on the respective potential-energy surfaces. The calculated energies in the gas phase include zero-point energy (ZPE) corrections and refer to 0 K. The natural atomic charges were calculated by natural population analysis.<sup>58</sup> We have also performed some of the calculations at the M06 level of theory for comparison,<sup>59</sup> and the values can be found in the [Supporting Information](#).

The infrared photodissociation spectra were measured with the ISORI instrument.<sup>60</sup> The instrument has the same ESI source as the LCQ instrument and the ionization conditions were analogous as mentioned above. The ionic complexes were mass-selected by the quadrupole mass filter and trapped in a cryo-cooled wire quadrupole ion trap (operated at 3 K, helium buffer gas). The ions cooled down in collisions with helium and ultimately formed loosely bound helium-tagged complexes. Afterward, the trapped ions were irradiated by photon pulses from an optical parametric oscillator/amplifier (OPO, 10 Hz). Finally, the ions were extracted from the trap, mass-analyzed by the second quadrupole mass filter, and the number of helium-tagged complexes ( $N$ ) was determined by a dynode/multiplier detector operated in ion-counting mode. In the following cycle, the light from the OPO was blocked by a

mechanical shutter, giving the number of unirradiated ions ( $N_0$ ). The infrared photodissociation spectroscopy (IRPD) spectra are constructed as the wavenumber dependence of  $(1 - N/N_0)$ .

## RESULTS AND DISCUSSION

The aim of this paper is to compare binding energies of silver and gold cations with various unsaturated hydrocarbons in  $\pi$ -complexes. Complexes of basic alkenes and alkynes such as ethylene and acetylene were addressed previously.<sup>61,62</sup> We have already studied  $\pi$ -complexes of [Au(PMe<sub>3</sub>)]<sup>+</sup> with unsaturated hydrocarbons.<sup>34</sup> We have shown that both the type of the multiple bond and its substitution have a large effect on the binding energies. Due to this fact, we decided to study an extended library of  $\pi$ -ligands as well as to include representatives of allenes, which are commonly applied in both gold and silver catalysis.

**Experimental BDEs.** First, we started with the investigation of the BDEs of the silver complexes. The ESI of a dichloromethane solution of AgSbF<sub>6</sub>, PPh<sub>3</sub>, and a hydrocarbon led to a mixture of silver complexes in the gas phase ([Figure 1a](#)). In every case, the most abundant ions were [Ag(PPh<sub>3</sub>)(H<sub>2</sub>O)]<sup>+</sup>, whereas the targeted complexes [Ag(PPh<sub>3</sub>)( $\pi$ -ligand)]<sup>+</sup> were detected with only a low intensity. Subsequently we mass-selected the <sup>107</sup>Ag isotopomers and performed the energy-resolved CID experiments. We have observed a single fragmentation channel—the loss of the hydrocarbon, followed by the immediate partial association of the [Ag(PPh<sub>3</sub>)]<sup>+</sup> fragment with background water molecules within the ion trap ([Figure 1b](#)). Calibration of the collision energy (see [S1](#)) and the evaluation of the energy onset of the fragmentation as depicted in [Figure 1c](#) provided the experimental binding energies of the [Ag(PPh<sub>3</sub>)]<sup>+</sup> cation with various  $\pi$ -ligands. [Table 1](#) summarizes these results.

The determined BDEs range from 1.35 to 1.64 eV. The smallest binding energies correspond to the binding of 1-pentene, benzene, and 1,1-dimethylallene. The largest binding energies were found for the complex of 1,5-cyclooctadiene (COD) (1.64 eV), followed by the complex of tetramethylallene (1.52 eV) and 2-pentyne (1.50 eV). In general, the binding energies of aliphatic mono-alkenes to [Ag(PPh<sub>3</sub>)]<sup>+</sup> clustered around 1.40 eV (with the exception of 1-pentene, see [Table 1](#), entries 1–5 and 9). In comparison, the binding energy of cyclooctene is larger (1.48 eV), which is probably due to a higher strain in the eight-membered ring.<sup>34</sup> Cycloalkenes with six- and eight-membered rings (except COD) have basically the same binding energies (1.44–1.45 eV); therefore, the binding does not depend on the ring size and conjugation. The significantly different value of 1,5-cyclooctadiene showed that there is an additional effect, which we discuss below in the paragraph concerning theoretical calculations. The binding energy of an alkene compared to that of an alkyne with the same substitution is about 0.1 eV smaller (from the comparison of 1-pentene with 1-pentyne and *cis/trans*-pentene with 2-pentyne).

For a direct comparison, we decided to investigate the corresponding gold  $\pi$ -complexes. We kept the experimental conditions as similar as possible.<sup>64,65</sup> Both the source and the subsequent MS/MS spectra exhibited comparable trends as in the case of the experiments with silver (see the [Supporting Information](#) for details). The results are also listed in [Table 1](#).

The determined interaction binding energies between the  $\pi$ -ligands and [Au(PPh<sub>3</sub>)]<sup>+</sup> were generally 0.2–0.3 eV larger than

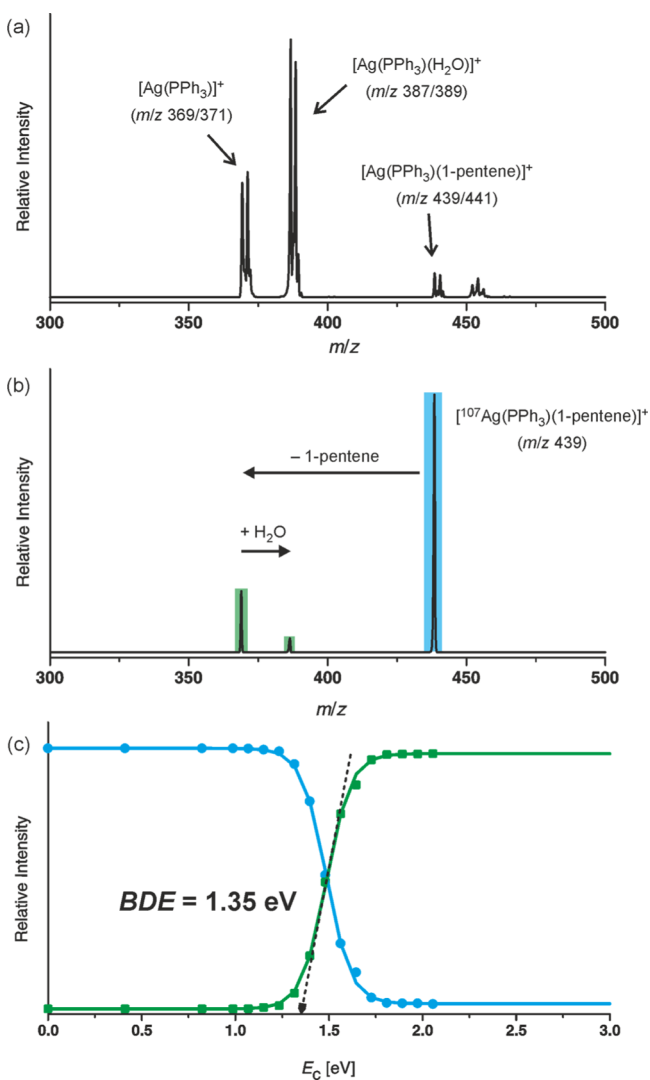


**Figure 1.** Determination of the experimental BDE of 1-pentene in the  $\pi$ -complex  $[\text{Ag}(\text{PPh}_3)(1\text{-pentene})]^+$ . (a) ESI-MS spectrum of dichloromethane solution of  $\text{AgSbF}_6$ ,  $\text{PPh}_3$ , and 1-pentene. (b) CID spectrum of the mass-selected cationic  $\pi$ -complex  $[\text{Ag}(\text{PPh}_3)(1\text{-pentene})]^+$  showing also the subsequent association of  $[\text{Ag}(\text{PPh}_3)]^+$  with the background water molecules. (c) Energy-resolved CID spectrum and the extrapolation of the fragmentation onset to determine the BDE.

the binding energies with  $[\text{Ag}(\text{PPh}_3)]^+$  and 0.2 eV lower than those with  $[\text{Au}(\text{PMe}_3)]^+$ , which were determined previously.<sup>34</sup> The  $\text{PMe}_3$  ligand is more electron-donating than  $\text{PPh}_3$ ; therefore,  $[\text{Au}(\text{PMe}_3)]^+$  should be less electrophilic than  $[\text{Au}(\text{PPh}_3)]^+$ .<sup>66</sup> The fact that  $[\text{Au}(\text{PMe}_3)]^+$  binds stronger with  $\pi$ -ligands than  $[\text{Au}(\text{PPh}_3)]^+$  points to the importance of  $\pi$ -backbonding. We note that the same trend of the effect of triphenylphosphine and trimethylphosphine was found for gold carbonyl complexes.<sup>67,68</sup> The binding energies in  $[\text{Au}(\text{PPh}_3)(\pi\text{-ligand})]^+$  ranged from 1.46 eV for benzene to 1.79 eV for the complex with tetramethylallene. The gold complexes do not show as significant dependence on the substitution and the type of the multiple bond as the silver complexes as most of them cluster around 1.65 eV. However, there are some exceptions: the internal alkyne (2-pentyne) binds with an energy of 1.77 eV. The binding energy of  $[\text{Au}(\text{PPh}_3)]^+$  with cyclooctene was higher than that with

aliphatic alkenes, similar to that found for the silver analogue. In addition, this value is as high as the binding energy of COD.

The direct comparison of the experimental values for the gold and the silver complexes is shown in Figure 2a. There is seemingly a linear correlation between the binding energies of  $\pi$ -ligands in the gold- and in the silver complexes. However, there are two visible outliers—the complexes with benzene and 1,5-cyclooctadiene—to which the silver cation binds much stronger compared to the other unsaturated hydrocarbons. This is discussed with the aid of theoretical calculations below.

**Theoretical BDEs.** Next, we turned our attention to the theoretical calculations. We performed density functional theory (DFT) calculations at the mPW1PW91/cc-pVTZ:LanL2DZ level of theory including ZPE and the BSSE corrections to determine the theoretical BDEs (Table 1). We also used the M06/cc-pVTZ/LanL2DZ level of theory including ZPE and BSSE corrections for the comparison—the results are in the Supporting Information (Table S1).

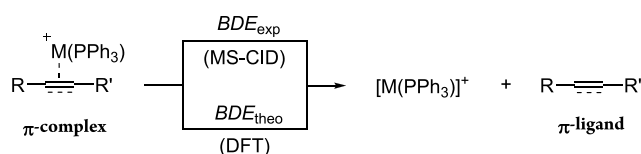
In the absolute values, the DFT predicted energies are on an average 0.3 eV smaller for the silver species and 0.2 eV smaller for the gold species compared to the experimental results. We observed the same difference between the experimental and theoretical values for the gold trimethylphosphino complexes in the previous study.<sup>34</sup>

In relative terms, there is a very good agreement with the trends found experimentally (Figure 2b-d). For the silver complexes, the weakest interactions were predicted to be with benzene, *trans*-pentene, 1-pentene, and 1,1-dimethylallene—three of four of these complexes were determined as the weakest by the MS experiment as well (Table 1). In addition, DFT predicts the strongest interaction between  $[\text{Ag}(\text{PPh}_3)]^+$  and COD, also in agreement with the experiment (Table 1). The reason for this becomes evident from the calculated structure (Figure 3): the silver cation interacts symmetrically with both double C–C bonds. This is not the case for the complexes with 1,3-cyclooctadiene and 1,3-cyclohexadiene and 1,4-cyclohexadiene. The differences among the theoretical binding energies are smaller than in the experiment; most of the theoretical binding energies cluster around 1.10 eV. Strikingly, the mPW1PW91/cc-pVTZ/LanL2DZ calculations fail to correctly describe the interaction with tetramethylallene, which was determined as the second strongest from the experiment.

For the  $[\text{Au}(\text{PPh}_3)(\pi\text{-ligand})]^+$  complexes, the theory correctly predicts the lowest binding energy for benzene and the largest binding energies for 2-pentyne, cyclooctene, and tetramethylallene. The theoretical binding energy of the gold cation with benzene is similar to the interactions of the silver cation with some of the  $\pi$ -ligands, which correlates well with the experiment. For the benzene complexes, the employed level of theory predicts the  $\eta^2$  coordination rather than the  $\eta^6$  coordination for both the silver and the gold complexes (see Figure 3).<sup>69</sup>

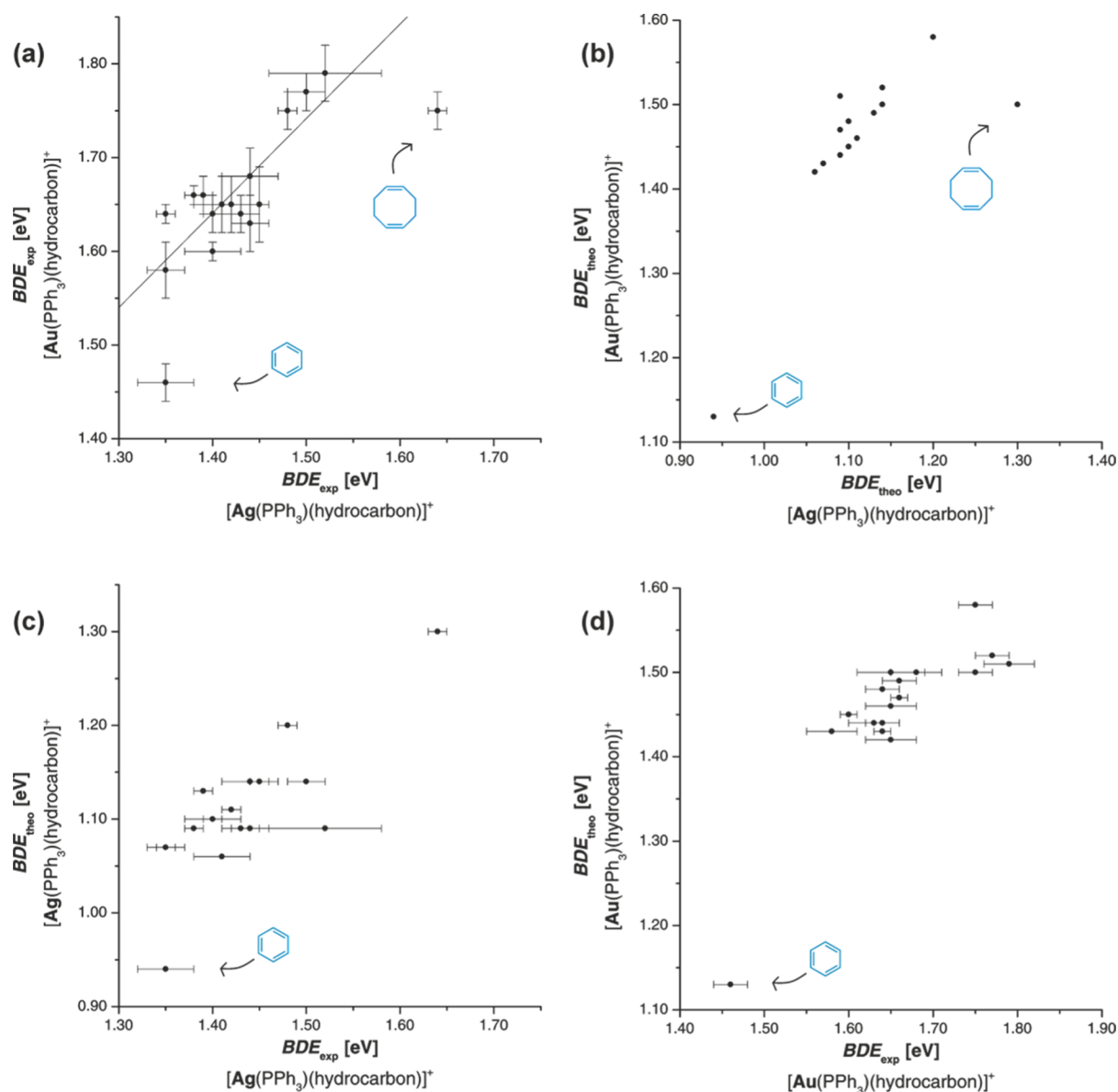
**Realistic Model Situation for Silver Cations.** The results reported above for the triphenylphosphino-silver(I) complexes do not properly illustrate a plausible situation in the solution because silver salts are added to reaction mixtures without an ancillary ligand—the first most probable reaction is the solvation of silver cation by molecules of the solvent. Because of this, we tried to determine the interaction of  $\pi$ -ligands with silver(I) cations with an additional ligand consisting of a solvent molecule, namely, dichloromethane, methanol, and acetonitrile. Unfortunately, we were unsuccessful

Table 1. Experimental and Theoretical Binding Energies of  $[M(PPh_3)]^+$  with Unsaturated Hydrocarbons in the  $[M(PPh_3)(Hydrocarbon)]^+$   $\pi$ -Complexes in the Gas Phase ( $M = Ag/Au$ )<sup>63</sup>



Entry	$\pi$ -Ligand	$BDE_{exp}$ [eV]		$BDE_{theo}$ [eV] <sup>a</sup>	
		M = Ag	M = Au	M = Ag	M = Au
1	1-pentene	1.35 ± 0.02	1.58 ± 0.03	1.07	1.43
2	cis-pentene	1.40 ± 0.01	1.64 ± 0.02	1.10	1.48
3	trans-pentene	1.41 ± 0.03	1.65 ± 0.03	1.06	1.42
4	2-methyl-1-butene	1.39 ± 0.01	1.66 ± 0.02	1.13	1.49
5	2-methyl-2-butene	1.38 ± 0.01	1.66 ± 0.01	1.09	1.47
6	1-pentyne	1.43 ± 0.02	1.64 ± 0.02	1.09	1.44
7	2-pentyne	1.50 ± 0.02	1.77 ± 0.02	1.14	1.52
8	benzene	1.35 ± 0.03	1.46 ± 0.02	0.94	1.13
9	styrene	1.40 ± 0.03	1.60 ± 0.01	1.10	1.45
10	phenylacetylene	1.42 ± 0.01	1.65 ± 0.03	1.11	1.46
11	cyclooctene	1.48 ± 0.01	1.75 ± 0.02	1.20	1.58
12	1,3-cyclooctadiene	1.44 ± 0.03	1.68 ± 0.03	1.14	1.50
13	1,5-cyclooctadiene	1.64 ± 0.01	1.75 ± 0.02	1.30	1.50
14	1,3-cyclohexadiene	1.45 ± 0.01	1.65 ± 0.04	1.14	1.50
15	1,4-cyclohexadiene	1.44 ± 0.02	1.63 ± 0.03	1.09	1.44
16	tetramethylallene	1.52 ± 0.06	1.79 ± 0.03	1.09	1.51
17	1,1-dimethylallene	1.35 ± 0.01	1.64 ± 0.01	1.07	1.43

<sup>a</sup>Calculations were performed at the mPW1PW91/cc-pVTZ/LanL2DZ level of theory and include ZPE and BSSE corrections.



**Figure 2.** (a,b) Correlation of the (a) experimental and (b) calculated binding energies of the silver and gold triphenylphosphine complexes with  $\pi$ -ligands with two visible outliers marked (benzene and COD). (c,d) Correlation of the experimental and calculated binding energies of the (c) silver and (d) gold triphenylphosphine complexes with  $\pi$ -ligands (benzene as an outlier marked).

ful in most cases because the desired  $\pi$ -complexes were presented with either only small intensity or not at all, and therefore we could not conduct CID experiments to determine their binding energies. However, in the case of using acetonitrile, it was possible to determine experimental BDEs for some of the  $\pi$ -complexes. We note that the  $[\text{Ag}(\text{CH}_3\text{CN})(\pi\text{-ligand})]^+$  complexes were generated from the dichloromethane solutions of  $\text{AgSbF}_6$  and the hydrocarbon with a minimal addition of acetonitrile (see the [Supporting Information](#) for details). If the concentration of acetonitrile was too large, the only detected ions were the  $[\text{Ag}(\text{CH}_3\text{CN})_2]^+$  ions.

Figure 4 shows a comparison of the fragmentation patterns of  $[\text{Ag}(\text{CH}_3\text{CN})(1\text{-pentene})]^+$  and  $[\text{Ag}(\text{CH}_3\text{CN})(\text{COD})]^+$ . The former dominantly eliminates 1-pentene, whereas the latter exclusively loses acetonitrile. Complexes with other hydrocarbons showed a similar fragmentation pattern to  $[\text{Ag}(\text{CH}_3\text{CN})(1\text{-pentene})]^+$ . This demonstrates that the

binding energy of acetonitrile to the silver cation is on the order of or larger than the binding energies of most of the  $\pi$ -ligands; only the binding energy of COD exceeds the binding energy of acetonitrile.

The experimentally determined results of the interaction of  $[\text{Ag}(\text{CH}_3\text{CN})]^+$  with selected unsaturated hydrocarbons are shown in [Table 2](#). The measured values for the interaction of the unsaturated hydrocarbons with  $[\text{Ag}(\text{CH}_3\text{CN})]^+$  were approximately 0.3 eV larger than those with  $[\text{Ag}(\text{PPh}_3)]^+$ . In addition, the values were similar to the binding energies in  $[\text{Au}(\text{PPh}_3)(\pi\text{-ligand})]^+$  (see [Table 1](#)). We also determined these values theoretically by the DFT calculations. The predicted values were shown to be approximately 0.15 eV smaller compared to the experimental values. On the other hand, the theoretical binding energies of the  $\pi$ -ligands in  $[\text{Au}(\text{PPh}_3)(\pi\text{-ligand})]^+$  and  $[\text{Ag}(\text{CH}_3\text{CN})(\pi\text{-ligand})]^+$  were predicted to be basically the same, which again agrees well with the experiment.

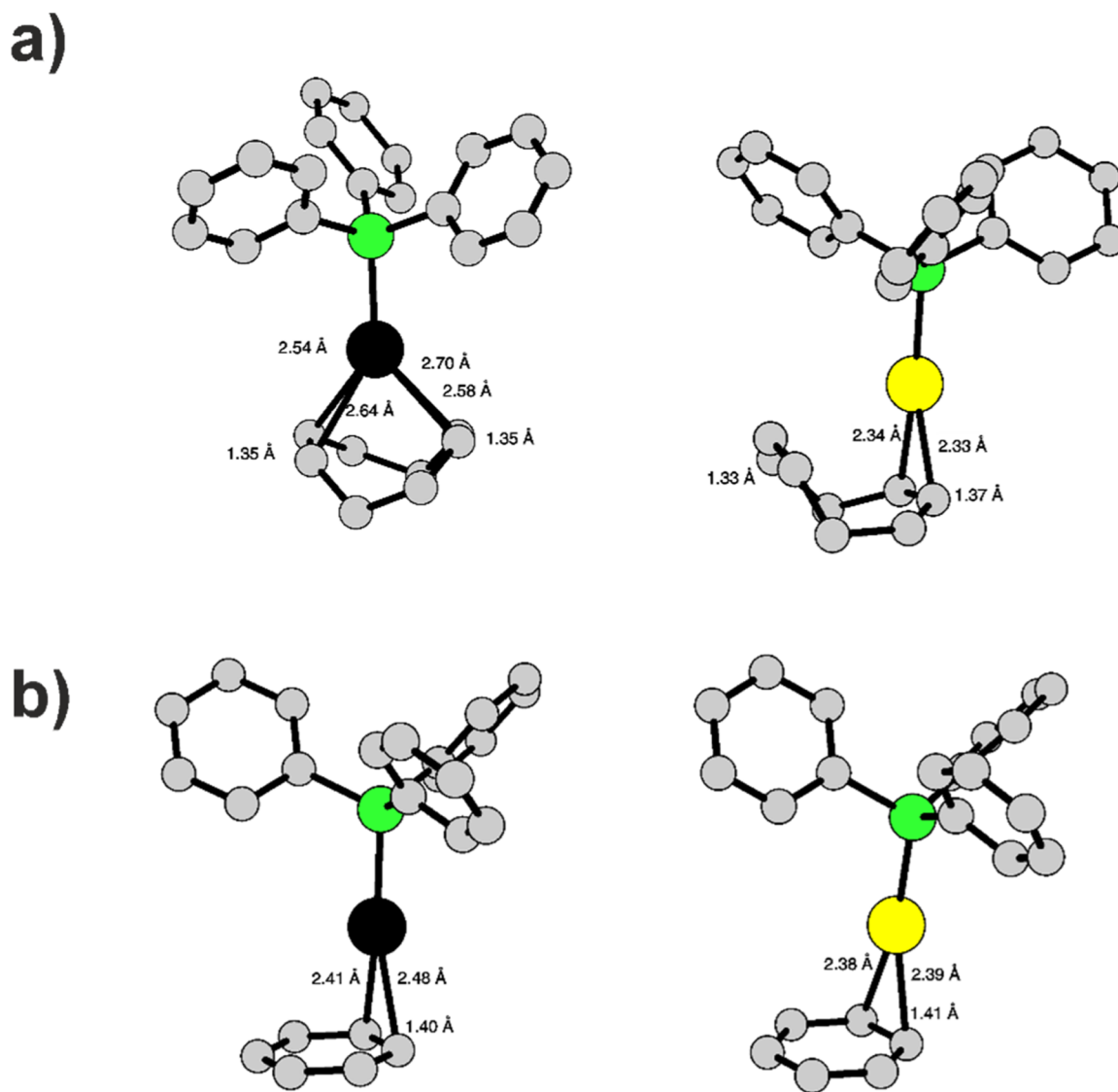


**Figure 3.** Optimized structures of the Ag/Au-triphenylphosphine  $\pi$ -complexes with (a) COD and (b) benzene at the mPW1PW91/cc-pVTZ/LanL2DZ level of theory. Coloring of the atoms: C, gray; P, green; Ag, black; and Au, yellow. The hydrogen atoms were removed for clarity.

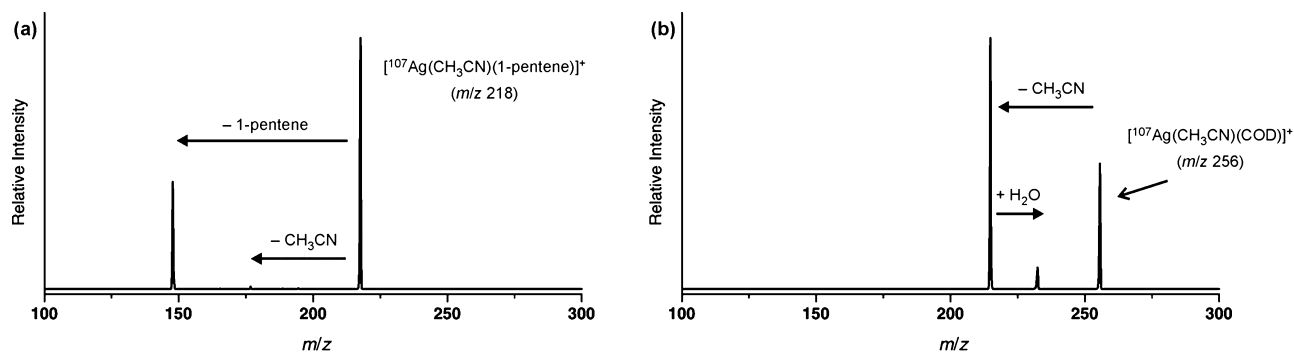


**Figure 4.** CID MS spectra of dichloromethane solution of  $\text{AgSbF}_6$ ,  $\text{CH}_3\text{CN}$ , and (a) 1-pentene or (b) COD.

We observed a competitive elimination of the hydrocarbon and acetonitrile from  $[\text{Ag}(\text{CH}_3\text{CN})(\pi\text{-ligand})]^+$ ; therefore, we could have extracted the binding energies for acetonitrile as well. The binding energies of acetonitrile in all the investigated complexes were about 1.7 eV and they were about the same as the binding energies of the  $\pi$ -ligands. However, the elimination of the hydrocarbons from  $[\text{Ag}(\text{CH}_3\text{CN})(\pi\text{-ligand})]^+$  largely

prevailed. It probably points to a kinetic preference of the  $\pi$ -ligand elimination.

**Infrared Photodissociation Spectroscopy.** Photodissociation spectroscopy provides IR or UV/Vis spectra of mass-selected ions.<sup>70–72</sup> We used IRPD spectroscopy to link the binding energies with the changes of the structure of the carbon–carbon multiple bonds.<sup>73</sup> The stretching frequency of

Table 2. Experimental and Theoretical Binding Energies of  $[\text{Ag}(\text{CH}_3\text{CN})]^+$  with Unsaturated Hydrocarbons in the Gas Phase<sup>63</sup>

Entry	$\pi$ -Ligand	$BDE_{\text{exp}}$ (hydrocarbon) [eV]	$BDE_{\text{theo}}$ (hydrocarbon) [eV] <sup>a</sup>	$BDE_{\text{exp}}$ ( $\text{CH}_3\text{CN}$ ) [eV]
1	1-pentene	$1.65 \pm 0.05$	1.47	$1.66 \pm 0.06$
2	2-methyl-1-butene	$1.69 \pm 0.05$	1.53	$1.71 \pm 0.09$
3	2-methyl-2-butene	$1.66 \pm 0.07$	1.49	$1.67 \pm 0.13$
4	styrene	$1.69 \pm 0.06$	1.49	$1.71 \pm 0.05$
5	cyclooctene	$1.71 \pm 0.05$	1.62	$1.67 \pm 0.05$

<sup>a</sup>Calculations were performed at the mPW1PW91/cc-pVTZ/LanL2DZ level of theory and include ZPE and BSSE corrections.

the unsaturated C–C bonds in the gold and silver  $\pi$ -complexes should correlate with their bond length and thus could be directly compared to their activation. We chose 2-pentyne as an example of the internal alkyne and measured IR spectra for both (triphenylphosphino)silver and (triphenylphosphino)gold  $\pi$ -complexes with 2-pentyne (Figure 5).

The  $\text{C}\equiv\text{C}$  stretching band of the  $[\text{Ag}(\text{PPh}_3)(2\text{-pentyne})]^+$  complex is located at  $2162\text{ cm}^{-1}$  (Figure 5b). The exchange of the silver cation by the gold cation leads to a clear red shift of the vibration (Figure 5a). However, the region of the  $\text{C}\equiv\text{C}$  stretching band contains two bands rather than just one, 2122 and  $2137\text{ cm}^{-1}$ , respectively. Most likely, the weaker band at  $2122\text{ cm}^{-1}$  is a combination band; hence, the  $\text{C}\equiv\text{C}$  stretching is at  $2137\text{ cm}^{-1}$  (see also S42 in the Supporting Information).

**Discussion.** The BDEs provide a good insight into the plausibility of the formation of the  $\pi$ -complexes and the degree of the activation of the multiple C–C bond in the complexes.<sup>34</sup> As to the plausibility of the formation of the complexes, the binding energies of the substrate molecules to the catalysts should be larger than those of the solvent molecules. We have shown that for likely the strongest interacting solvent molecule, acetonitrile, the formation of silver complexes with  $\pi$ -ligands versus with acetonitrile can be in competition. We do not need to consider the competition between the gold and silver complexes because the metals are used only in catalytic amounts (normally around 5–10%), which means that the unsaturated hydrocarbons are in a large excess and therefore the gold and the silver species do not compete for them.

The second objective is the comparison of the degree to which the silver and gold ions activate an unsaturated bond. We can follow several parameters to assess the activation, for example, the lengthening of the C–C unsaturated bond or the charge on the unsaturated C–C bond in the  $\pi$ -complexes.<sup>74</sup> For the silver complexes, we chose to include also various

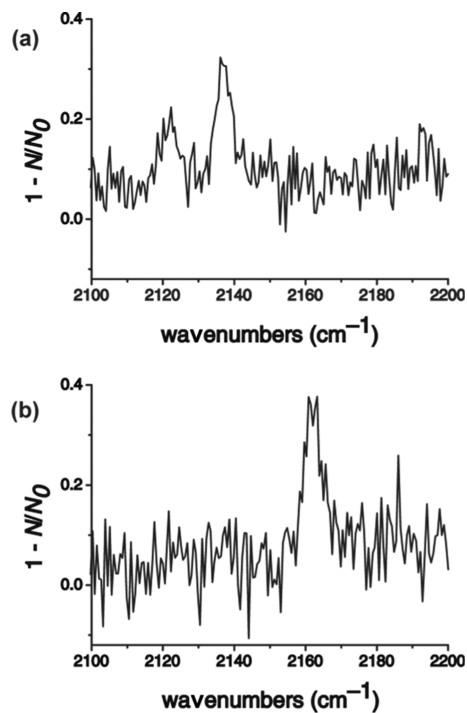


Figure 5. Experimental IR of (a) gold-triphenylphosphine (b) and silver-triphenylphosphine  $\pi$ -complexes with 2-pentyne in the gas phase.

ancillary ligands to simulate the solvent, namely, acetonitrile, methanol, dichloromethane, and water.

First, we analyzed the length of the unsaturated bond in the  $\pi$ -complexes in the gas phase (Table 3). By this measure, gold is expected to activate the unsaturated bonds more effectively

Table 3. Unsaturated Bond Length in Gold and Silver  $\pi$ -Complexes in the Gas Phase

Type	$\pi$ -Ligand	$d(\text{C1-C2}) [\text{\AA}]^a$						
		free	L=Au(PPh <sub>3</sub> )	L=Ag(PPh <sub>3</sub> )	L=Ag(CH <sub>3</sub> CN)	L=Ag(CH <sub>2</sub> Cl <sub>2</sub> )	L=Ag(CH <sub>3</sub> OH)	L=Ag(H <sub>2</sub> O)
Terminal alkene	(1-pentene) 	1.325	1.365	1.352	1.358	1.359	1.360	1.361
Internal alkene	(cis-pentene) 	1.329	1.371	1.358	1.365	1.366	1.368	1.368
Terminal alkyne	(1-pentyne) 	1.199	1.223	1.215	1.219	1.219	1.220	1.221
Internal alkyne	(2-pentyne) 	1.201	1.227	1.218	1.222	1.223	1.224	1.224
Allene	(1,1-dimethylallene) 	1.300	1.342	1.327	1.335	1.335	1.337	1.337

<sup>a</sup>Calculations were performed at the mPW1PW91/cc-pVTZ/LanL2DZ level of theory.

Table 4. Calculated Natural Atomic Charges in the Gold and Silver  $\pi$ -Complexes in the Gas Phase (UH Corresponds to an Unsaturated Hydrocarbon)

Type	$\pi$ -Ligand	Natural atomic charges <sup>a,b</sup>					
		L=Au(PPh <sub>3</sub> )	L=Ag(PPh <sub>3</sub> )	L=Ag(CH <sub>3</sub> CN)	L=Ag(CH <sub>2</sub> Cl <sub>2</sub> )	L=Ag(CH <sub>3</sub> OH)	L=Ag(H <sub>2</sub> O)
Terminal alkene	(1-pentene) 	C1: -0.48 (-0.00)	C1: -0.49 (-0.02)	C1: -0.50 (-0.02)	C1: -0.50 (-0.02)	C1: -0.50 (-0.02)	C1: -0.50 (-0.02)
		C2: -0.15 (+0.08)	C2: -0.13 (+0.09)	C2: -0.13 (+0.09)	C2: -0.14 (+0.08)	C2: -0.14 (+0.08)	C2: -0.14 (+0.09)
		L: +0.86	L: +0.87	L: +0.86	L: +0.86	L: +0.86	L: +0.86
		UH: +0.14	UH: +0.13	UH: +0.14	UH: +0.14	UH: +0.14	UH: +0.14
Internal alkene	(cis-pentene) 	C1: -0.22 (+0.01)	C1: -0.22 (+0.00)	C1: -0.23 (+0.01)	C1: -0.22 (+0.00)	C1: -0.23 (+0.00)	C1: -0.23 (+0.01)
		C2: -0.21 (+0.02)	C2: -0.21 (+0.01)	C2: -0.22 (+0.01)	C2: -0.22 (+0.00)	C2: -0.22 (+0.00)	C2: -0.22 (+0.01)
		L: +0.84	L: +0.87	L: +0.87	L: +0.87	L: +0.87	L: +0.86
		UH: +0.16	UH: +0.13	UH: +0.13	UH: +0.13	UH: +0.13	UH: +0.14
Terminal alkyne	(1-pentyne) 	C1: -0.34 (-0.05)	C1: -0.35 (-0.06)	C1: -0.37 (-0.08)	C1: -0.37 (-0.08)	C1: -0.38 (-0.09)	C1: -0.38 (-0.09)
		C2: +0.07	C2: +0.06	C2: +0.06	C2: +0.06	C2: +0.09	C2: +0.07
		L: +0.87	L: +0.90	L: +0.90	L: +0.91	L: +0.89	L: +0.91
		UH: +0.13	UH: +0.10	UH: +0.10	UH: +0.09	UH: +0.11	UH: +0.09
Internal alkyne	(2-pentyne) 	C1: -0.03	C1: -0.04	C1: -0.05	C1: -0.05	C1: -0.06	C1: -0.05
		C2: -0.04	C2: -0.05	C2: -0.06	C2: -0.06	C2: -0.04	C2: -0.06
		L: +0.87	L: +0.91	L: +0.91	L: +0.91	L: +0.89	L: +0.90
		UH: +0.13	UH: +0.09	UH: +0.09	UH: +0.09	UH: +0.11	UH: +0.10
Allene	(1,1-dimethylallene) 	C1: -0.55 (-0.04)	C1: -0.57 (-0.10)	C1: -0.59 (-0.08)	C1: -0.58 (-0.08)	C1: -0.59 (-0.08)	C1: -0.59 (-0.08)
		C2: +0.03	C2: +0.06	C2: +0.05	C2: +0.05	C2: +0.04	C2: +0.05
		L: +0.86	L: +0.88	L: +0.87	L: +0.87	L: +0.88	L: +0.87
		UH: +0.14	UH: +0.12	UH: +0.13	UH: +0.13	UH: +0.12	UH: +0.13

<sup>a</sup>Calculations were performed at the mPW1PW91/cc-pVTZ/LanL2DZ level of theory. <sup>b</sup>Values in brackets correspond to a sum with directly attached hydrogen atoms.

as the gold provided the largest lengthening of the unsaturated bond in all complexes. For silver species, the lengthening was most profound for the complexes of water–silver and methanol–silver compared to the complexes with triphenylphosphine–silver having the smallest effect.

Second, we calculated the natural atomic charges in the  $\pi$ -complexes by natural population analysis. The aim is to correlate the activation of the unsaturated bonds for a nucleophilic attack with the delocalization of the charge from the metals to the unsaturated bond (Table 4). There are no big differences in charge delocalization among the complexes. The overall positive charge on the  $\pi$ -ligands ranged from 0.13 to 0.16 e in the gold complexes and these values dropped by only of 0.01–0.04 e for the corresponding silver complexes. The bigger differences (on the side of 0.04 e) were found in charge distributions in complexes with alkynes.

Overall, the population analysis suggests that the charge delocalization might be a part of the activation of the  $\pi$ -ligands in gold and silver complexes. However, the differences in C–C bond distances of these ligands in the gold and silver complexes attest that the  $\pi$ -back-bonding probably plays a more important role in the activation of the ligands than the positive charge.<sup>75,76</sup> This conclusion is in agreement with results obtained for silver(I) and gold(I) complexes bearing bidentate phosphine ligands. These complexes bind strongly with  $\pi$ -ligands, leading to significant C–C bond elongations.<sup>44</sup>

## CONCLUSIONS

We determined the binding energies of various cationic silver(I) and gold(I)  $\pi$ -complexes in the gas phase experimentally and theoretically. The results show that for the same ancillary ligand PPh<sub>3</sub>, gold(I) binds stronger to unsaturated hydrocarbons than silver(I). The same trend was also confirmed spectroscopically by measuring vibrational frequencies of the C≡C bond in [Au(PPh<sub>3</sub>)(2-pentyne)]<sup>+</sup> and [Ag(PPh<sub>3</sub>)(2-pentyne)]<sup>+</sup>. When a different supporting ligand on silver is used to simulate the conditions in a reaction mixture, where silver is likely coordinated to a solvent molecule, silver can bind to the  $\pi$ -ligands as strongly as gold. However, the activation of the  $\pi$ -ligands is always slightly smaller, measured by the prolongation of the unsaturated bond and the positive charge delocalization.

The results thus suggest that  $\pi$ -bonds in unsaturated hydrocarbons can be likely activated for nucleophilic attack by both ligated gold cations and solvated silver cations if both cations are present in a reaction mixture. Many reaction parameters can affect which mode of activation prevails for the reaction outcome. The reactivity of one or the other cation can be disfavored by steric effects, counterion effects, solvation effects, and other factors.<sup>27,77</sup>

## ASSOCIATED CONTENT

### Supporting Information

The Supporting Information is available free of charge at <https://pubs.acs.org/doi/10.1021/acs.organomet.1c00143>.

Experimental details, MS and MS/MS spectra, energy resolved CID experiments and energies (PDF)

Optimized structures of all compounds in XYZ coordinates (ZIP)

## AUTHOR INFORMATION

### Corresponding Authors

Petr Motloch – Jesus College, Cambridge CB5 8BL, U.K.;  
orcid.org/0000-0002-3118-4119; Email: pm567@cantab.ac.uk

Jana Roithová – Department of Spectroscopy and Catalysis, Institute for Molecules and Materials, Radboud University Nijmegen, AJ Nijmegen 135 6525, The Netherlands;  
orcid.org/0000-0001-5144-0688; Email: J.Roithova@science.ru.nl

### Author

Juraj Jašík – J. Heyrovský Institute of Physical Chemistry of the CAS, Prague 8 182 23, Czech Republic

Complete contact information is available at:

<https://pubs.acs.org/10.1021/acs.organomet.1c00143>

### Notes

The authors declare no competing financial interest.

## ACKNOWLEDGMENTS

Previous address for all authors is Department of Organic Chemistry, Faculty of Science, Charles University in Prague, Prague 2, 128 43, Czech Republic, where the experimental part of the work was conducted. The authors gratefully acknowledge the financial support from the European Research Council.

## REFERENCES

- (1) Hashmi, A. S. K.; Hutchings, G. J. Gold Catalysis. *Angew. Chem., Int. Ed.* **2006**, *45*, 7896–7936.
- (2) Gorin, D. J.; Toste, F. D. Relativistic effects in homogeneous gold catalysis. *Nature* **2007**, *446*, 395–403.
- (3) Hashmi, A. S. K. Gold-Catalyzed Organic Reactions. *Chem. Rev.* **2007**, *107*, 3180–3211.
- (4) Hashmi, A. S. K.; Rudolph, M. Gold catalysis in total synthesis. *Chem. Soc. Rev.* **2008**, *37*, 1766–1775.
- (5) Rudolph, M.; Hashmi, A. S. K. Gold catalysis in total synthesis—an update. *Chem. Soc. Rev.* **2012**, *41*, 2448–2462.
- (6) Friend, C. M.; Hashmi, A. S. K. Gold Catalysis. *Acc. Chem. Res.* **2014**, *47*, 729–730.
- (7) Hashmi, A. S. K. Dual Gold Catalysis. *Acc. Chem. Res.* **2014**, *47*, 864–876.
- (8) Zhang, L. A Non-Diazo Approach to  $\alpha$ -Oxo Gold Carbenes via Gold-Catalyzed Alkyne Oxidation. *Acc. Chem. Res.* **2014**, *47*, 877–888.
- (9) Wang, Y.-M.; Lackner, A. D.; Toste, F. D. Development of Catalysts and Ligands for Enantioselective Gold Catalysis. *Acc. Chem. Res.* **2014**, *47*, 889–901.
- (10) Obradors, C.; Echavarren, A. M. Gold-Catalyzed Rearrangements and Beyond. *Acc. Chem. Res.* **2014**, *47*, 902–912.
- (11) Zhang, D.-H.; Tang, X.-Y.; Shi, M. Gold-Catalyzed Tandem Reactions of Methylene-cyclopropanes and Vinylidene-cyclopropanes. *Acc. Chem. Res.* **2014**, *47*, 913–924.
- (12) Fürstner, A. From Understanding to Prediction: Gold- and Platinum-Based  $\pi$ -Acid Catalysis for Target Oriented Synthesis. *Acc. Chem. Res.* **2014**, *47*, 925–938.
- (13) Alcaide, B.; Almendros, P. Gold-Catalyzed Cyclization Reactions of Allenol and Alkynol Derivatives. *Acc. Chem. Res.* **2014**, *47*, 939–952.
- (14) Fensterbank, L.; Malacria, M. Molecular Complexity from Polyunsaturated Substrates: The Gold Catalysis Approach. *Acc. Chem. Res.* **2014**, *47*, 953–965.
- (15) Yeom, H.-S.; Shin, S. Catalytic Access to  $\alpha$ -Oxo Gold Carbenes by N–O Bond Oxidants. *Acc. Chem. Res.* **2014**, *47*, 966–977.

- (16) Hashmi, A. S. K. Homogeneous Gold Catalysis Beyond Assumptions and Proposals—Characterized Intermediates. *Angew. Chem., Int. Ed.* **2010**, *49*, 5232–5241.
- (17) Pernpointner, M.; Hashmi, A. S. K. Fully Relativistic, Comparative Investigation of Gold and Platinum Alkyne Complexes of Relevance for the Catalysis of Nucleophilic Additions to Alkynes. *J. Chem. Theory Comput.* **2009**, *5*, 2717–2725.
- (18) Brooner, R. E. M.; Widenhoefer, R. A. Cationic, Two-Coordinate Gold  $\pi$  Complexes. *Angew. Chem., Int. Ed.* **2013**, *52*, 11714–11724.
- (19) Lauterbach, T.; Asiri, A. M.; Hashmi, A. S. K. Organometallic Intermediates of Gold Catalysis. *Adv. Organomet. Chem.* **2014**, *62*, 261–297.
- (20) Jones, A. C. Gold  $\pi$ -Complexes as Model Intermediates in Gold Catalysis. In *Homogeneous Gold Catalysis*; Slaughter, L. M., Ed.; Springer International Publishing: Cham, 2015, pp 133–165.
- (21) Jašíková, L.; Anania, M.; Hybelbauerová, S.; Roithová, J. Reaction Intermediates Kinetics in Solution Investigated by Electro-spray Ionization Mass Spectrometry: Diaurated Complexes. *J. Am. Chem. Soc.* **2015**, *137*, 13647–13657.
- (22) Wang, D.; Cai, R.; Sharma, S.; Jirak, J.; Thummanapelli, S. K.; Akhmedov, N. G.; Zhang, H.; Liu, X.; Petersen, J. L.; Shi, X. “Silver Effect” in Gold(I) Catalysis: An Overlooked Important Factor. *J. Am. Chem. Soc.* **2012**, *134*, 9012–9019.
- (23) Homs, A.; Escofet, I.; Echavarren, A. M. On the Silver Effect and the Formation of Chloride-Bridged Digold Complexes. *Org. Lett.* **2013**, *15*, 5782–5785.
- (24) Zhu, Y.; Day, C. S.; Zhang, L.; Hauser, K. J.; Jones, A. C. A Unique Au–Ag–Au Triangular Motif in a Trimetallic Halonium Dication: Silver Incorporation in a Gold(I) Catalyst. *Chem.—Eur. J.* **2013**, *19*, 12264–12271.
- (25) Lu, Z.; Han, J.; Hammond, G. B.; Xu, B. Revisiting the Influence of Silver in Cationic Gold Catalysis: A Practical Guide. *Org. Lett.* **2015**, *17*, 4534–4537.
- (26) Zhdanko, A.; Maier, M. E. Explanation of “Silver Effects” in Gold(I)-Catalyzed Hydroalkoxylation of Alkynes. *ACS Catal.* **2015**, *5*, 5994–6004.
- (27) Jia, M.; Bandini, M. Counterion Effects in Homogeneous Gold Catalysis. *ACS Catal.* **2015**, *5*, 1638–1652.
- (28) Yang, Y.; Antoni, P.; Zimmer, M.; Sekine, K.; Mulks, F. F.; Hu, L.; Zhang, L.; Rudolph, M.; Rominger, F.; Hashmi, A. S. K. Dual Gold/Silver Catalysis Involving Alkynylgold(III) Intermediates Formed by Oxidative Addition and Silver-Catalyzed C–H Activation for the Direct Alkynylation of Cyclopropenes. *Angew. Chem., Int. Ed.* **2019**, *58*, 5129–5133.
- (29) Hu, L.; Dieltl, M. C.; Han, C.; Rudolph, M.; Rominger, F.; Hashmi, A. S. K. Au–Ag Bimetallic Catalysis Providing 3-Alkynyl Benzofurans from Phenols via Tandem C–H Alkynylation/Oxy-Alkynylation. *Angew. Chem., Int. Ed.* **2021**, *60*, 106337–10642.
- (30) Škríba, A.; Jašíková, L.; Roithová, J. Silver(I) and gold(I) complexes of diethylmalonate. *Int. J. Mass Spectrom.* **2012**, *330*–332, 226–232.
- (31) Jašíková, L.; Roithová, J. Interaction of Gold Acetylides with Gold(I) or Silver(I) Cations. *Organometallics* **2013**, *32*, 7025–7033.
- (32) Schröder, D. Applications of Electrospray Ionization Mass Spectrometry in Mechanistic Studies and Catalysis Research. *Acc. Chem. Res.* **2012**, *45*, 1521–1532.
- (33) Roithová, J.; Janková, Š.; Jašíková, L.; Váňa, J.; Hybelbauerová, S. Gold–Gold Cooperation in the Addition of Methanol to Alkynes. *Angew. Chem., Int. Ed.* **2012**, *51*, 8378–8382.
- (34) Jašíková, L.; Roithová, J. Interaction of the Gold(I) Cation Au(PMe<sub>3</sub>)<sup>+</sup> with Unsaturated Hydrocarbons. *Organometallics* **2012**, *31*, 1935–1942.
- (35) Schulz, J.; Jašíková, L.; Škríba, A.; Roithová, J. Role of Gold(I)  $\alpha$ -Oxo Carbenes in the Oxidation Reactions of Alkynes Catalyzed by Gold(I) Complexes. *J. Am. Chem. Soc.* **2014**, *136*, 11513–11523.
- (36) Dorel, R.; Echavarren, A. M. Gold(I)-Catalyzed Activation of Alkynes for the Construction of Molecular Complexity. *Chem. Rev.* **2015**, *115*, 9028–9072.
- (37) Zuccaccia, D.; Belpassi, L.; Tarantelli, F.; Macchioni, A. Ion Pairing in Cationic Olefin–Gold(I) Complexes. *J. Am. Chem. Soc.* **2009**, *131*, 3170–3171.
- (38) Brooner, R. E. M.; Brown, T. J.; Widenhoefer, R. A. Synthesis and Study of Cationic, Two-Coordinate Triphenylphosphine–Gold– $\pi$  Complexes. *Chem.—Eur. J.* **2013**, *19*, 8276–8284.
- (39) Motloch, P.; Blahut, J.; Císaršová, I.; Roithová, J. X-ray characterization of triphenylphosphine-gold(I) olefin  $\pi$ -complexes and the revision of their stability in solution. *J. Organomet. Chem.* **2017**, *848*, 114–117.
- (40) Shapiro, N. D.; Toste, F. D. Synthesis and structural characterization of isolable phosphine coinage metal  $\pi$ -complexes. *Proc. Natl. Acad. Sci. U.S.A.* **2008**, *105*, 2779–2782.
- (41) Hooper, T. N.; Green, M.; McGrady, J. E.; Patel, J. R.; Russell, C. A. Synthesis and structural characterisation of stable cationic gold(i) alkene complexes. *Chem. Commun.* **2009**, 3877–3879.
- (42) Zhu, Y.; Day, C. S.; Jones, A. C. Synthesis and Structure of Cationic Phosphine Gold(I) Enol Ether Complexes. *Organometallics* **2012**, *31*, 7332–7335.
- (43) Grirrane, A.; Álvarez, E.; Albero, J.; García, H.; Corma, A. Multinuclear silver(i) XPhos complexes with cyclooctatetraene: photochemical C–C bond cleavage of acetonitrile and cyanide bridged Ag cluster formation. *Dalton Trans.* **2016**, *45*, 5444–5450.
- (44) Griebel, C.; Hodges, D. D.; Yager, B. R.; Liu, F. L.; Zhou, W.; Makaravage, K. J.; Zhu, Y.; Norman, S. G.; Lan, R.; Day, C. S.; Jones, A. C. Bis(biphenyl) Phosphines: Structure and Synthesis of Gold(I) Alkene  $\pi$ -Complexes with Variable Phosphine Donicity and Enhanced Stability. *Organometallics* **2020**, *39*, 2665–2671.
- (45) Ridlen, S. G.; Wu, J.; Kulkarni, N. V.; Dias, H. V. R. Isolable Ethylene Complexes of Copper(I), Silver(I), and Gold(I) Supported by Fluorinated Scorpionates [HB{3-(CF<sub>3</sub>),5-(CH<sub>3</sub>)Pz}3]<sup>–</sup> and [HB{3-(CF<sub>3</sub>),5-(Ph)Pz}3]<sup>–</sup>. *Eur. J. Inorg. Chem.* **2016**, *2016*, 2573–2580.
- (46) Klimovica, K.; Kirschbaum, K.; Daugulis, O. Synthesis and Properties of “Sandwich” Diimine-Coinage Metal Ethylene Complexes. *Organometallics* **2016**, *35*, 2938–2943.
- (47) Navarro, M.; Toledo, A.; Joost, M.; Amgoune, A.; Mallet-Ladeira, S.; Bourissou, D.  $\pi$  Complexes of  $\text{PP}$  and  $\text{PN}$  chelated gold(i). *Chem. Commun.* **2019**, *55*, 7974–7977.
- (48) Navarro, M.; Toledo, A.; Mallet-Ladeira, S.; Sosa Carrizo, E. D.; Miqueu, K.; Bourissou, D. Versatility and adaptative behaviour of the  $\text{PN}$  chelating ligand MeDalpos within gold(i)  $\pi$  complexes. *Chem. Sci.* **2020**, *11*, 2750–2758.
- (49) Zins, E.-L.; Pepe, C.; Schröder, D. Energy-dependent dissociation of benzylpyridinium ions in an ion-trap mass spectrometer. *J. Mass Spectrom.* **2010**, *45*, 1253–1260.
- (50) Hanzlová, E.; Váňa, J.; Shaffer, C. J.; Roithová, J.; Martinů, T. Evidence for the Cyclic CN<sub>2</sub> Carbene in the Gas Phase. *Org. Lett.* **2014**, *16*, 5482–5485.
- (51) Škríba, A.; Schulz, J.; Roithová, J. Monitoring of Reaction Intermediates in the Gas Phase: Ruthenium-Catalyzed C–C Coupling. *Organometallics* **2014**, *33*, 6868–6878.
- (52) Hývl, J.; Roithová, J. Mass Spectrometric Studies of Reductive Elimination from Pd(IV) Complexes. *Org. Lett.* **2014**, *16*, 200–203.
- (53) Frisch, M. J.; Trucks, G. W.; Schlegel, H. B.; Scuseria, G. E.; Robb, M. A.; Cheeseman, J. R.; Scalmani, G.; Barone, V.; Mennucci, B.; Petersson, G. A.; Nakatsuji, H.; Caricato, M.; Li, X.; Hratchian, H. P.; Izmaylov, A. F.; Bloino, J.; Zheng, G.; Sonnenberg, J. L.; Hada, M.; Ehara, M.; Toyota, K.; Fukuda, R.; Hasegawa, J.; Ishida, M.; Nakajima, T.; Honda, Y.; Kitao, O.; Nakai, H.; Vreven, T.; Montgomery, J. A., Jr.; Peralta, J. E.; Ogliaro, F.; Bearpark, M. J.; Heyd, J.; Brothers, E. N.; Kudin, K. N.; Staroverov, V. N.; Kobayashi, R.; Normand, J.; Raghavachari, K.; Rendell, A. P.; Burant, J. C.; Iyengar, S. S.; Tomasi, J.; Cossi, M.; Rega, N.; Millam, N. J.; Klene, M.; Knox, J. E.; Cross, J. B.; Bakken, V.; Adamo, C.; Jaramillo, J.; Gomperts, R.; Stratmann, R. E.; Yazyev, O.; Austin, A. J.; Cammi, R.; Pomelli, C.; Ochterski, J. W.; Martin, R. L.; Morokuma, K.; Zakrzewski, V. G.; Voth, G. A.; Salvador, P.; Dannenberg, J. J.; Dapprich, S.; Daniels, A. D.; Farkas, Ö.; Foresman, J. B.; Ortiz, J. V.;

Cioslowski, J.; Fox, D. J. *Gaussian 09*; Gaussian, Inc.: Wallingford, CT, USA, 2009.

(54) Adamo, C.; Barone, V. Exchange functionals with improved long-range behavior and adiabatic connection methods without adjustable parameters: The mPW and mPW1PW models. *J. Chem. Phys.* **1998**, *108*, 664–675.

(55) Dunning, T. H. Gaussian basis sets for use in correlated molecular calculations. I. The atoms boron through neon and hydrogen. *J. Chem. Phys.* **1989**, *90*, 1007–1023.

(56) Hay, P. J.; Wadt, W. R. Ab initio effective core potentials for molecular calculations. Potentials for K to Au including the outermost core orbitals. *J. Chem. Phys.* **1985**, *82*, 299–310.

(57) Simon, S.; Duran, M.; Dannenberg, J. J. How does basis set superposition error change the potential surfaces for hydrogen-bonded dimers? *J. Chem. Phys.* **1996**, *105*, 11024–11031.

(58) Reed, A. E.; Weinstock, R. B.; Weinhold, F. Natural population analysis. *J. Chem. Phys.* **1985**, *83*, 735–746.

(59) Zhao, Y.; Truhlar, D. G. Density Functionals with Broad Applicability in Chemistry. *Acc. Chem. Res.* **2008**, *41*, 157–167.

(60) Jašík, J.; Žabka, J.; Roithová, J.; Gerlich, D. Infrared spectroscopy of trapped molecular dications below 4K. *Int. J. Mass Spectrom.* **2013**, *354–355*, 204–210.

(61) Barnett, N. J.; Slipchenko, L. V.; Gordon, M. S. The Binding of Ag<sup>+</sup> and Au<sup>+</sup> to Ethene. *J. Phys. Chem. A* **2009**, *113*, 7474–7481.

(62) Dias, H. V. R.; Flores, J. A.; Wu, J.; Kroll, P. Monomeric Copper(I), Silver(I), and Gold(I) Alkyne Complexes and the Coinage Metal Family Group Trends. *J. Am. Chem. Soc.* **2009**, *131*, 11249–11255.

(63) It has to be noted that we do not present these experimental values as accurate thermodynamic ones. However, by our research, we show that these easily obtained results are in a very good agreement with accurate mass spectrometry techniques as well as commonly used reasonably advanced theoretical calculations (see previously mentioned references from our group and references therein). When these values are determined under the same experimental conditions, they can be used for comparison within the group, but they cannot be used for benchmarking theoretical calculations. We have noticed that these results tend to be shifted as a group, similarly to the case of using different theoretical methods and basis sets.

(64) Gabelica, V.; Pauw, E. D. Internal energy and fragmentation of ions produced in electrospray sources. *Mass Spectrom. Rev.* **2005**, *24*, 566–587.

(65) Di Marco, V. B.; Bombi, G. G. Electrospray mass spectrometry (ESI-MS) in the study of metal–ligand solution equilibria. *Mass Spectrom. Rev.* **2006**, *25*, 347–379.

(66) Suresh, C. H.; Koga, N. Quantifying the Electronic Effect of Substituted Phosphine Ligands via Molecular Electrostatic Potential. *Inorg. Chem.* **2002**, *41*, 1573–1578.

(67) Gatineau, D.; Lesage, D.; Clavier, H.; Dossmann, H.; Chan, C. H.; Milet, A.; Memboeuf, A.; Cole, R. B.; Gimbert, Y. Bond dissociation energies of carbonyl gold complexes: a new descriptor of ligand effects in gold(i) complexes? *Dalton Trans.* **2018**, *47*, 15497–15505.

(68) Dias, H. V. R.; Dash, C.; Yousufuddin, M.; Celik, M. A.; Frenking, G. Cationic Gold Carbonyl Complex on a Phosphine Support. *Inorg. Chem.* **2011**, *50*, 4253–4255.

(69) Bayler, A.; Schier, A.; Bowmaker, G. A.; Schmidbauer, H. Gold Is Smaller than Silver. Crystal Structures of [Bis(trimesitylphosphine)-gold(I)] and [Bis(trimesitylphosphine)silver(I)] Tetrafluoroborate. *J. Am. Chem. Soc.* **1996**, *118*, 7006–7007.

(70) Roithová, J. Characterization of reaction intermediates by ion spectroscopy. *Chem. Soc. Rev.* **2012**, *41*, 547–559.

(71) Roithová, J.; Gray, A.; Andris, E.; Jašík, J.; Gerlich, D. Helium Tagging Infrared Photodissociation Spectroscopy of Reactive Ions. *Acc. Chem. Res.* **2016**, *49*, 223–230.

(72) Jašíková, L.; Roithová, J. Infrared Multiphoton Dissociation Spectroscopy with Free-Electron Lasers: On the Road from Small Molecules to Biomolecules. *Chem.—Eur. J.* **2018**, *24*, 3374–3390.

(73) Škríba, A.; Jašík, J.; Andris, E.; Roithová, J. Interaction of Ruthenium(II) with Terminal Alkynes: Benchmarking DFT Methods with Spectroscopic Data. *Organometallics* **2016**, *35*, 990–994.

(74) Schmidbauer, H.; Schier, A. Gold  $\eta^2$ -Coordination to Unsaturated and Aromatic Hydrocarbons: The Key Step in Gold-Catalyzed Organic Transformations. *Organometallics* **2010**, *29*, 2–23.

(75) Nechaev, M. S.; Rayón, V. M.; Frenking, G. Energy Partitioning Analysis of the Bonding in Ethylene and Acetylene Complexes of Group 6, 8, and 11 Metals: (CO)<sub>5</sub>TM–C<sub>2</sub>H<sub>x</sub> and Cl<sub>4</sub>TM–C<sub>2</sub>H<sub>x</sub> (TM = Cr, Mo, W), (CO)<sub>4</sub>TM–C<sub>2</sub>H<sub>x</sub> (TM = Fe, Ru, Os), and TM<sup>+</sup>–C<sub>2</sub>H<sub>x</sub> (TM = Cu, Ag, Au). *J. Phys. Chem. A* **2004**, *108*, 3134–3142.

(76) Ziegler, T.; Rauk, A. A theoretical study of the ethylene-metal bond in complexes between copper(1+), silver(1+), gold(1+), platinum(0) or platinum(2+) and ethylene, based on the Hartree-Fock-Slater transition-state method. *Inorg. Chem.* **1979**, *18*, 1558–1565.

(77) Lu, Z.; Li, T.; Mudshinge, S. R.; Xu, B.; Hammond, G. B. Optimization of Catalysts and Conditions in Gold(I) Catalysis—Counterion and Additive Effects. *Chem. Rev.* **2021**, DOI: 10.1021/acs.chemrev.0c00713.